ChemInform Abstract: Chromium-Doped Germanium Clusters CrGen (n = 1—5): Geometry, Electronic Structure, and Topology of Chemical Bonding

ARTICLE *in* THE JOURNAL OF PHYSICAL CHEMISTRY A · JANUARY 2008

Impact Factor: 2.69 · DOI: 10.1021/jp0773233 · Source: PubMed

Chromium-Doped Germanium Clusters $CrGe_n$ ($n = 1-5$): Geometry, Electronic Structure, and Topology of Chemical Bonding

Xin-Juan Hou,[†] G. Gopakumar,[†] Peter Lievens,[‡] and Minh Tho Nguyen*[,†]

Department of Chemistry and Institute for Nanoscale Physics and Chemistry, University of Leuven, Celestijnenlaan 200F, B-3001 Leuven, Belgium, and Laboratory of Solid State Physics and Magnetism and Institute for Nanoscale Physics and Chemistry, University of Leuven, Celestijnenlaan 200D, B-3001 Leuven, Belgium

Received: September 12, 2007

The structure and properties of small neutral and cationic $CrGe_n^{0,+}$ clusters, with n from 1 to 5, were investigated using quantum chemical calculations at the CASSCF/CASPT2 and DFT/B3LYP levels. Smaller clusters prefer planar geometries, whereas the lowest-lying electronic states of the neutral $CrGe_4$, $CrGe_5$, and cationic $CrGe_5^+$ forms exhibit nonplanar geometries. Most of the clusters considered prefer structures with high-spin ground state and large magnetic moments. Relative to the values obtained for the pure Ge_n clusters, fragmentation energies of doped $CrGe_n$ clusters are smaller when n is 3 and 4 and larger when $n = 5$. The averaged binding energy tends to increase with the increasing number of Ge atoms. For $n = 5$, the binding energies for Ge_5, $CrGe_5$, and $CrGe_5^+$ are similar to each other, amounting to ~2.5 eV. The Cr atom acts as a general electron donor in neutral $CrGe_n$ clusters. Electron localization function (ELF) analyses suggest that the chemical bonding in chromium-doped germanium clusters differs from that of their pure or Li-doped counterparts and allow the origin of the inherent high-spin ground state to be understood. The differential ΔELF picture, obtained in separating both α and β electron components, is consistent with that derived from spin density calculations. For $CrGe_n$, $n = 2$ and 3, a small amount of d−π back-donation is anticipated within the framework of the proposed bonding model.

Introduction

Silicon clusters have widely been studied because they are important for the fine processing of semiconductors and the synthesis of novel materials. The encapsulation of transition metals in the silicon clusters has been demonstrated to change the structures and properties of Si_n clusters.[1] For the heavier congeners in group IV, relatively little attention has been paid on the preparation and properties of metal-doped M_mGe_n clusters. The pure germanium clusters are chemically reactive and thus not suitable as a building block of self-assembly materials.[2] By an appropriate choice of the metal dopant, it is possible to design metallic as well as semiconducting nanotubes using Ge_n as building blocks.[3] Metal-encapsulated caged clusters of Ge were investigated using the ab initio pseudopotential plane-wave method.[4] Their results revealed that metal-doped M_mGe_n clusters possess large HOMO−LUMO gaps. Electronic properties of silicon- and germanium-doped indium clusters were investigated by photoionization spectroscopy and photoelectron spectroscopy.[5] The geometries, stability, and electronic properties of Ge_n and $TMGe_n$ (TM = Zn, W, and Cu) clusters have also been systematically investigated by using a density functional approach.[6−8] The remarkable features of W-doped Ge_n clusters were distinctly different from those of Cu− and Ni−Ge_n clusters, indicating that the growth pattern of the TM−Ge_n depends on the kind of doped TM impurity. Recently, quantum chemical calculations on the structure and energies of lithiated diatomic germanium clusters and their cations (Li_nGe_2 and $Li_nGe_2^+$) revealed that they all have low-spin ground state.[9]

Small elemental and molecular clusters provide a bridge toward the understanding of how matter evolves from atoms to bulk.[10,11] The available experimental[12−18] and theoretical[19−26] studies on small Ge clusters focused mostly on the lowest energy electronic structure. Chromium has the largest magnetic moment among the 3d transition metal elements with half-filled 3d and 4s orbitals. In view of the recent experimental observations on the Cr-doped germanium clusters,[27] we set out to investigate the magnetic properties of these clusters employing various theoretical methodologies. As far as we are aware, there were no previous theoretical investigations on the $CrGe_n$ clusters. In the present paper, a detailed investigation on equilibrium geometries, stabilities, electronic structure, and bonding properties, in particular the topology of the electron densities, of Cr-doped germanium clusters are reported.

Computational Methods

Calculations were performed for all possible spin multiplicities $M = 2S + 1$ for each cluster considered. All investigated clusters were fully optimized making use of the density functional theory with the popular hybrid B3LYP functional,[28] in conjunction with a 6-311+G(d) basis set for chromium and the LANL2DZ*dp* basis set with an effective core potential (ECP) for germanium (denoted hereafter as B3LYP/Gen). The ECP[29] has been selected in view of the large number of structures investigated. For each spin manifold, the geometry optimization was carried out without any symmetry constraint at different

* Corresponding author. E-mail: minh.nguyen@chem.kuleuven.be.
[†] Department of Chemistry and Institute for Nanoscale Physics and Chemistry.
[‡] Laboratory of Solid State Physics and Magnetism and Institute for Nanoscale Physics and Chemistry.

10.1021/jp0773233 CCC: $37.00
Published on Web 12/04/2007

initial configurations. Harmonic vibrational frequencies were subsequently calculated to characterize the located stationary points as equilibrium structures having all real vibrational frequencies.

In order to calibrate the applied theoretical methodologies, some test calculations were carried out on Ge_2 using the B3LYP/LANL2DZ*dp* level. The predicted Ge−Ge bond length of 2.44 Å is comparable to the 2.42 Å obtained using a multireference configuration interaction method.[30] The bonding energies of Ge_n clusters predicted at the B3LYP/LANL2DZ*dp* level are 1.34, 1.93, 2.38, and 2.52 eV for $n = 2$, 3, 4, and 5, respectively. These values are in good agreement with the experimental values of 1.35, 2.04, 2.53, and 2.72 eV, respectively.[6] Accordingly, the error bars on the relative energies obtained in the present work are expected to be ±0.2 eV. All geometry optimizations were performed using the Gaussian 03 package.[31] The low-lying electronic states and leading electronic configurations of $CrGe_2$ are in good agreement with that derived at CASPT2/ANO-RCC level[32] and are reported in respective sections.

We also performed separate computations on some energetically low-lying isomers of the cationic $CrGe_4^+$ using the B3LYP functional and a larger triple-ζ basis set with polarization functions (TZ2P).[33] These computations were carried out using the Amsterdam density functional (ADF) software package.[34]

A natural population analysis (NPA) of a selection of low energetic isomers of neutral and cationic $CrGe_n$ ($n = 1 - 5$) was done in order to probe the bonding phenomena and the relative stabilities of the different structures for these clusters. As an additional attempt to understand the electronic structure, we considered the atoms-in-molecules (AIM) approach,[35] which is a useful tool providing valuable information about the structure and bonding in molecules. According to the AIM theory, a chemical bond is defined by the presence of a bond critical point (bcp), where the gradient of the electron density vanishes, and is characterized as a (3, −1) critical point. The electron density for the present AIM analysis was generated at the B3LYP/6-311++G(d,p) level, the critical points located and the bond paths plotted with the AIM2000 program package.[36] On the other hand, the electron localization function (ELF) analysis is a simple measure of localization in atomic and molecular systems.[37] The ELF value is always in the range of [0; 1], and 1 corresponds to a perfect localization. The zero-flux surfaces of the ELF separate the space to basins (Ω_i), which allow defining and calculating the properties of core, chemical bond, and lone pairs. There are two main types of basins: (i) core basins are located around nuclei and always occur when the atomic number is larger than 2, and (ii) valence basins are characterized by their synaptic orders, i.e., the number of core basins that share a common boundary surface with the valence basin. Monosynaptic basins represent the lone pairs, whereas disynaptic basins belong to the covalent bonds. The integral of the total electron density over Ω_i shows the population of the given basin.

In the present study, the AIM and ELF analyses have been carried out on the selected molecules, namely, $CrGe_2$ and $CrGe_3$, using the AIM2000[36] and TopMod[38] programs, respectively. The ELF isosurfaces and their cut planes were plotted using the graphical program gOpenMol.[39] To ensure the accuracy of basin integrations, a threshold value of 10^{-7} has been adopted. A parallel set of net charges was also obtained using the AIM methodology and will be presented in respective sections.

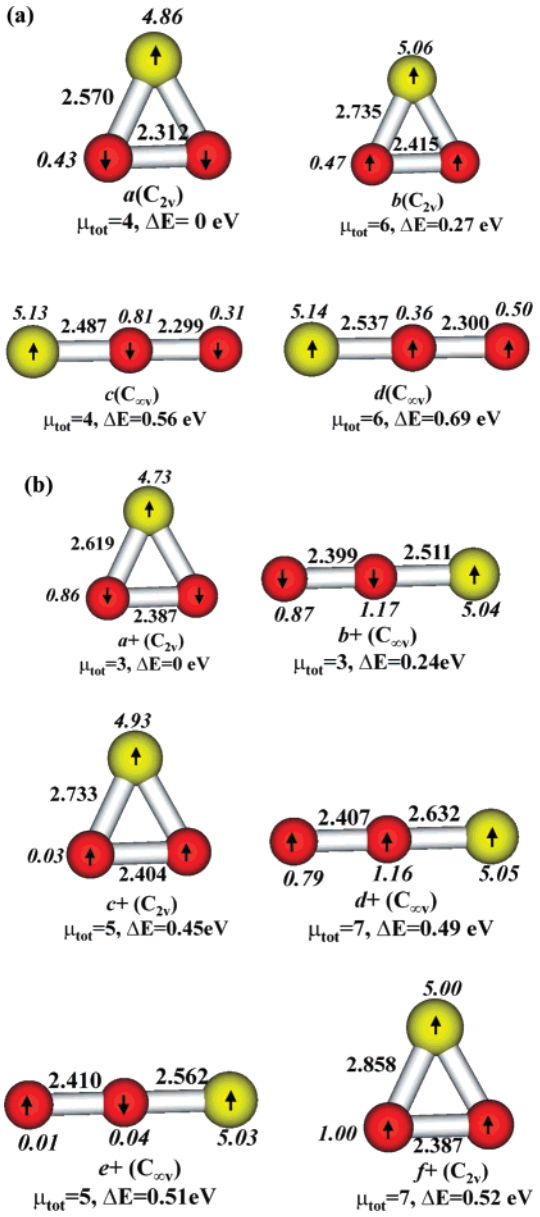

Figure 1. Geometries of the ground state and low-lying isomers of $CrGe_2$ (a) and $CrGe_2^+$ (b). Bond lengths are given in angstroms, local magnetic moments (in italics) in μ_B.

Results and Discussion

Neutral and Cationic $CrGe_n^{0,+}$ ($n = 1-5$) Clusters. The optimized geometries, electronic structures, magnetic moments, and relative energies of the energetically lower-lying isomers of the neutral and cationic $CrGe_n^{0,+}$ ($n = 1-5$) clusters calculated at the B3LYP/Gen level are given in Figures 1 −4. The magnetic moment of each structure is evaluated from its multiplicity: the spin magnetic moment is equal to the difference of spin-up and spin-down electrons. Our computations indicate that the most stable structure of $CrGe_n$ cluster, with n from 1 to 4 corresponds, to a high-spin quintet electronic state, whereas it is a septet state for $n = 5$. For $CrGe_n^+$ ($n = 1$, 4, and 5) clusters, the most stable structure corresponds to a sextet state, and a low-lying quartet state is derived for $n = 2$ and 3. An overview of the extended list of isomers located for these clusters in all possible $M = 2S + 1$ states can be found in the Supporting Information. The computed local magnetic moments for Cr and Ge atoms in the low-energy isomers are also shown, as italic numerals, in Figures 1−4.

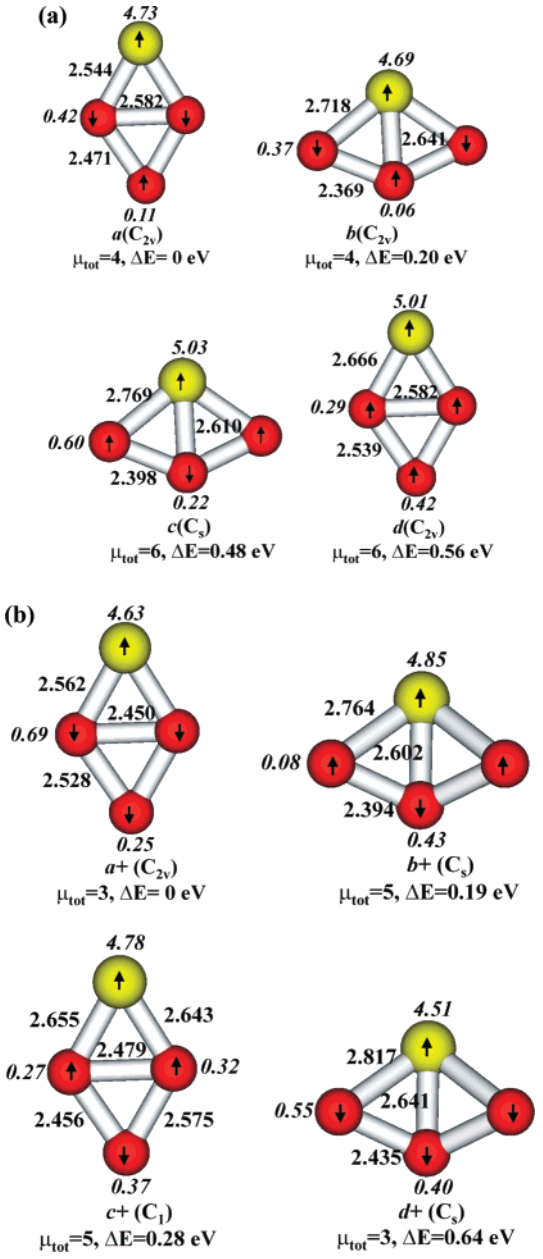

Figure 2. Geometries of the ground state and low-lying isomers of $CrGe_3$ (a) and $CrGe_3^+$ (b). Bond lengths are given in angstroms, local magnetic moments (in italics) in μ_B.

Size dependence for the atomic binding energies and the fragmentation energies of the $CrGe_n$ and $CrGe_n^+$ clusters are plotted in Figures 5 and 6. The natural charge populations, energy gaps between the highest singly occupied molecular orbitals (SOMO) and lowest unoccupied molecular orbitals (LUMO), and dipole moments for the ground state structures of $CrGe_n$ and $CrGe_n^+$ ($n = 1-5$) are listed in Table 1.

Equilibrium Structure and Magnetic Moment. *CrGe and CrGe*$^+$. The ground state of CrGe dimer is a quintet $^5\Pi$ state **a** and is different from the analogous WGe dimer for which a triplet ground $^3\Delta$ state has been derived. For CrGe the triplet electronic state **c** is an energetically higher-lying one as compared to the quintet ground state. Also note that the dimer in its septet state is 0.24 eV less stable than **a**. The lowest energy equilibrium structure of the cationic $CrGe^+$ corresponds to a $^6\Sigma$ state **a**+ with a bond distance of 2.585 Å. This is, indeed, slightly longer than the corresponding value of 2.516 Å in **a**. For isomer **a**, the Ge atom turns out to be ferromagnetic with respect to the Cr. For $CrGe^+$, the spin of Cr is antiparallel to the Ge, resulting in a total magnetic moment of 5 μ_B.

CrGe$_2$ *and CrGe*$_2^+$. Interaction of Ge_2 with one Cr atom leads to two distinct types of low-energy isomers, namely, a C_{2v} structure with Cr being on the C_2 axis and a linear Cr−Ge−Ge structure with $C_{\infty v}$ point group. The symmetrical linear structures of $D_{\infty h}$ symmetry in which the Cr atom equally connects two Ge atoms were energetically higher-lying for both the neutral and cation, $CrGe_2$ and $CrGe_2^+$. However, in the present study, we have concentrated mainly on the low-energy isomers. For $CrGe_2$ the C_{2v} symmetric $^5A_1$ state **a** has been assigned as the ground state. Isomer **b** possessing a septet $^7B_1$ state is being 0.27 eV above the quintet ground state, whereas the corresponding values of two linear isomers **c** and **d** with $C_{\infty v}$ symmetry are 0.56 and 0.69 eV, respectively.

As for $LiGe_2$, the ground state geometry also falls under the C_{2v} point group, but it is characterized as a doublet $^2B_1$ state. The geometrical change from the quintet ground state to the excited $^7B_1$ state is significant; the Ge−Cr and Ge−Ge distances increase by 0.165 and 0.10 Å, respectively. The electronic configurations of $CrGe_2$ at its $^5A_1$ and $^7B_1$ electronic states are as follows.

$^5A_1$: ...$(8a_1)^2(3b_2)^2(3b_1)^2(9a_1)^1(1a_2)^1(4b_1)^1(4b_2)^1$.

$^7B_1$: ...$(8a_1)^2(3b_2)^2(2b_1)^2(9a_1)^1(10a_1)^1(1a_2)^1(3b_1)^1(4b_1)^1(4b_2)^1$.

In order to confirm the reliability of the applied DFT methods, we used the more extended molecular orbital methodologies, in particular the complete active space CASSCF and the second-order perturbation theory CASPT2, in conjunction with the relativistic ANO-RCC and LANL2dz basis sets.[32] The predicted electronic configuration of $CrGe_2$ for the two low-lying electronic states agrees well with that derived at the CASPT2/ANO-RCC and CASSCF/LANL2DZdp levels.

The $^7B_1$ state results from an electronic excitation from the $3b_1$ orbital to the $10a_1$. The $3b_1$ and $10a_1$ molecular orbitals have considerable contributions from the Ge_2 π-bonding and antibonding MOs, respectively. It can be concluded that the geometrical change resulting in the elongation of the Ge−Ge bond is due to the occupancy of an electron in the antibonding MO.

Removal of an electron from $CrGe_2$ leads to the formation of $CrGe_2^+$ for which a quartet $^4B_1$ ground state **a**+ is derived. Two lower-lying isomers **c**+ and **f**+, each falls under the C_{2v} symmetry, and three linear isomers **b**+, **d**+, and **c**+ are calculated to be located 0.45, 0.52, 0.24, 0.49, and 0.51 eV above the ground state. The electronic configurations of $CrGe_2^+$ for the $^4B_1$ **a**+ and the $^6B_1$ **c**+ are the following.

$^4B_1$: ...$(8a_1)^2(3b_1)^2(3b_2)^2(9a_1)^1(1a_2)^1(4b_2)^1$.

$^6B_1$: ...$(8a_1)^2(2b_1)^2(3b_2)^2(9a_1)^1(1a_2)^1(3b_1)^1(4b_1)^1(4b_2)^1$.

The $^6B_1$ state is formed by electronic excitation from the $3b_1$ to the $4b_1$ orbital and corresponds, in other words, to a $\pi^* \leftarrow \pi$ transition.

For the ground state structures of both $CrGe_2$ and $CrGe_2^+$ species, the Cr atom bears an antiparallel spin with other two ferromagnetically coupled Ge atoms, yielding a total spin magnetic moment of 4 μ_B for $CrGe_2$ and 3 μ_B for $CrGe_2^+$, respectively. The $CrGe_2$ and $CrGe_2^+$ (both C_{2v} and $C_{\infty v}$) at higher manifolds have a ferromagnetic structure with a total magnetic moments of 6μ_B for **b** and **d** and 7μ_B for **d**+ and **f**+, respectively.

CrGe$_3$ *and CrGe*$_3^+$. We were able to derive high-spin ground states for both neutral and cationic $CrGe_3$ species. For the former it was the quintet $^5A_1$ state **a**, whereas a quartet $^4B_2$ state **a**+

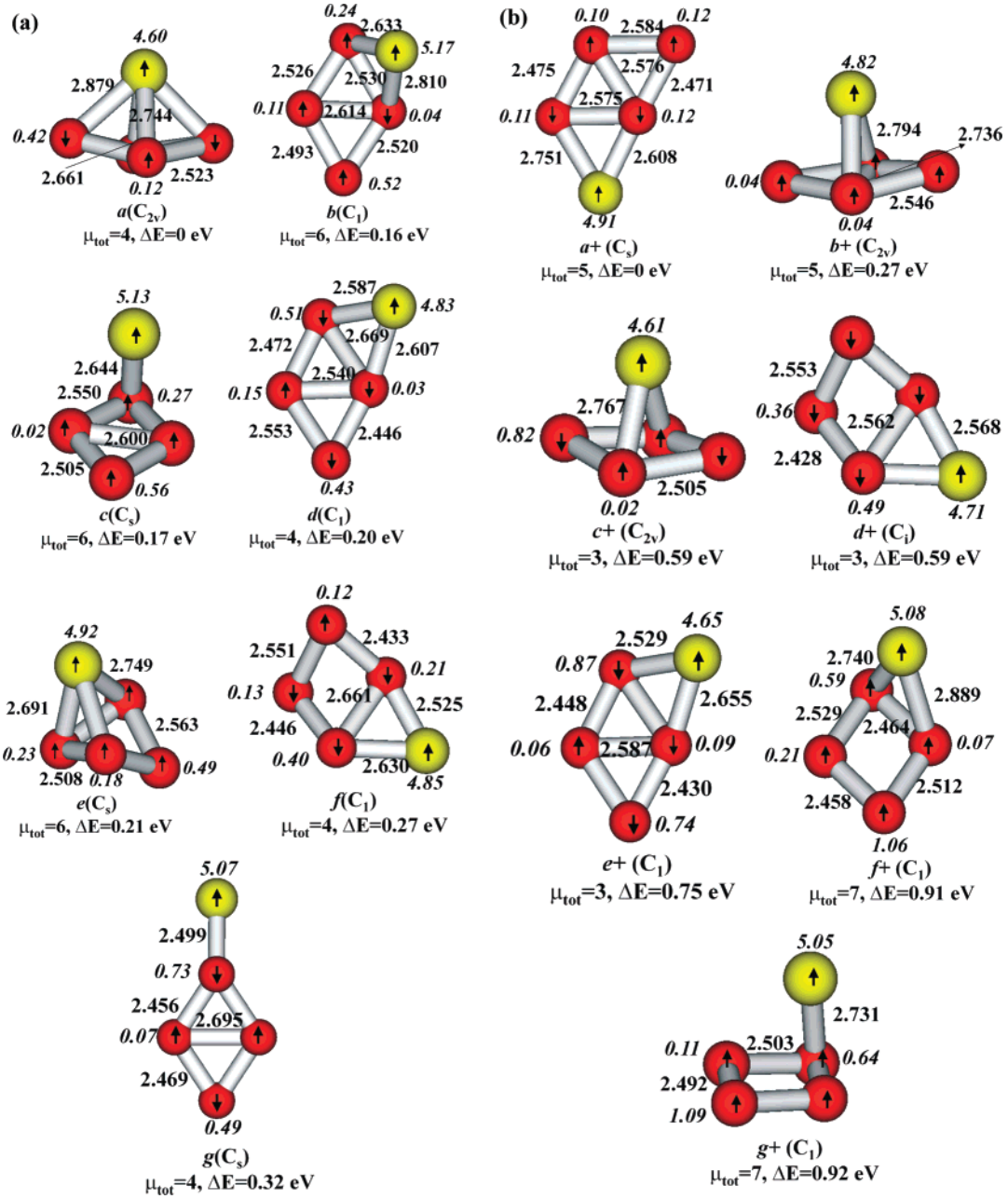

Figure 3. Geometries of the ground state and low-lying isomers of $CrGe_4$ (a) and $CrGe_4^+$ (b). Bond lengths are given in angstroms, local magnetic moments (in italics) in μ_B.

has been assigned for the latter, both having a C_{2v} point group symmetry. The electronic configuration of **a** and **a**+ are the following.

$^5A_1$: ...$(9a_1)^2(4b_2)^2(3b_1)^2(1a_2)^1(10a_1)^1(4b_1)^1(5b_2)^1$.

$^4B_2$: ...$(9a_1)^2(4b_2)^2(3b_1)^2(1a_2)^1(10a_1)^1(4b_1)^1$.

The cation is formed by removal of an electron from the b_2 orbital of the neutral molecule. The Ge−Ge bond length in $CrGe_3$ **a** is about 0.3 Å longer than the corresponding distance in $CrGe_2$, for the ground electronic state. It is found that the occupancy of the electron in the $p_x(\pi)$ orbital of the Ge_2 unit is 0.2 e less than that of the ground state of $CrGe_2$, leading to an apparent elongation of the Ge−Ge bond.

The electronic configuration of **d** is ...$(9a_1)^2(4b_2)^2(2b_1)^2(3b_1)^1$-$(1a_2)^1(10a_1)^1(4b_1)^1(11a_1)^1(5b_2)^1$, which results from the excitation of an electron from the $3b_1$ orbital to the $11a_1$ orbital, with respect to the MOs of **a**. The electronic states of the isomers **b** and **b**+, where the chromium atom binds with three germanium atoms, are $^5B_2$ and $^6A'$, respectively. These states lie energetically 0.20 and 0.19 eV above the corresponding ground states.

At this stage, it is interesting to compare the ground states of Cr-doped and W-doped Ge_3 clusters. Whereas the former has a planar geometry with a quintet ground state, the latter possesses a pyramidal structure and a singlet state. The planar rhombic structure of WGe_3 is an energetically higher-lying species with an energy gap of 1.92 eV with respect to the pyramidal structure. It could be noted that the most stable geometry of $CrGe_3$ resembles the $NiGe_3$ and $CuGe_3$ counterparts.

For **a**, the two Ge atoms, adjacent to the Cr, are actually ferromagnetically coupled with each other, whereas the third Ge is antiferromagnetically coupled with the Cr atom. On the contrary, for the cation **a**+, all three Ge atoms are ferromagnetically coupled with each other and antiferromagnetically coupled with Cr. For **b**, two terminal Ge atoms are antiferro-

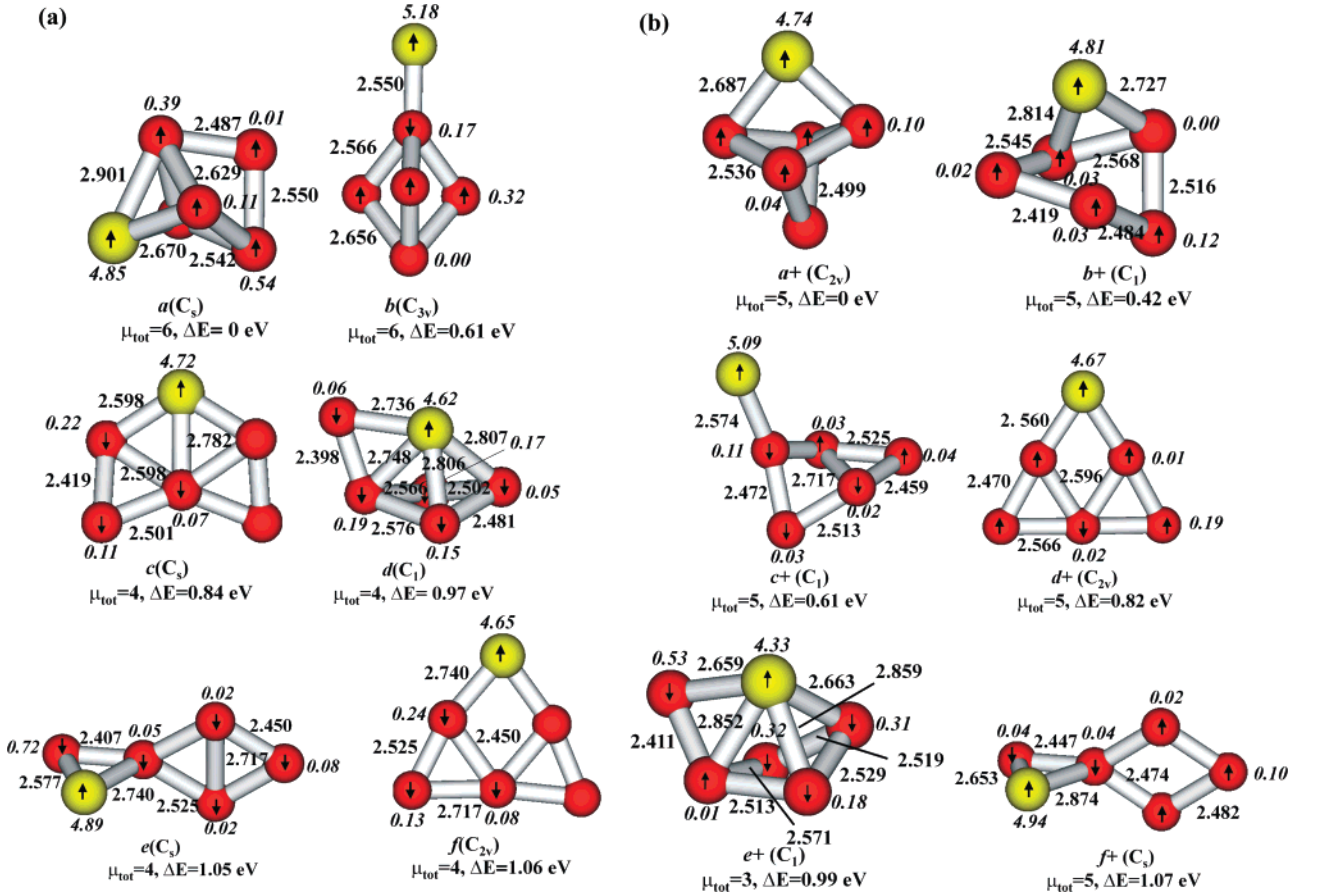

Figure 4. Geometries of the ground state and low-lying isomers of $CrGe_5$ (a) and $CrGe_5^+$ (b). Bond lengths are given in angstroms, local magnetic moments (in italics) in μ_B.

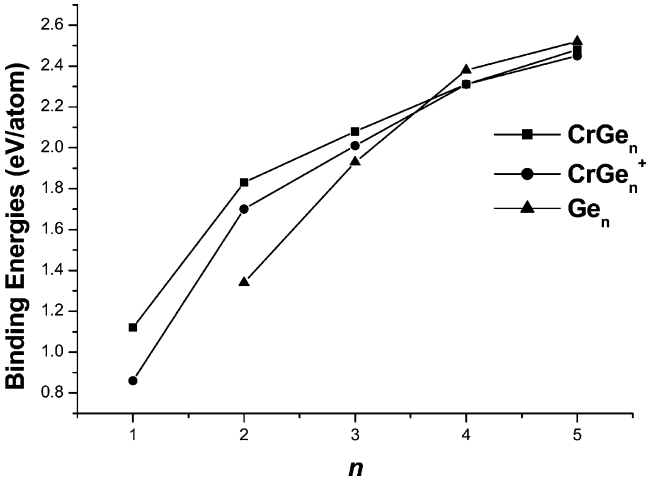

Figure 5. Size dependence of the atomic binding energies of the $CrGe_n$ and $CrGe_n^+$ ($n = 1-5$) clusters.

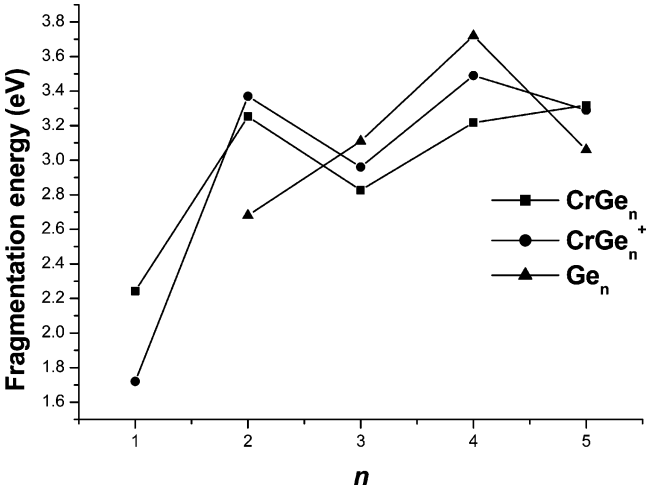

Figure 6. Size dependence of the fragmentation energies of the $CrGe_n$ and $CrGe_n^+$ ($n = 1-5$) clusters.

magnetically coupled with the third Ge and Cr atoms. Note that in the case of the **d**, all atoms are ferromagnetically coupled with each other.

$CrGe_4$ and $CrGe_4^+$. The $CrGe_4$ cluster was located to have a $^5B_2$ ground state having a C_{2v} pyramidal geometry, in which Cr occupies the apex. No planar low-energy isomer was located for $CrGe_4$. Several nonplanar isomers within the quintet or septet spin manifolds are located for $CrGe_4$ with energies being 0.1−0.3 eV above the ground state. For **a** the bridging Cr is coupled ferromagnetically with two Ge atoms, that have a spin polarization of 0.12 e, and antiferromagnetic with two Ge atoms that have a spin polarization of 0.42 e, yielding the total magnetic moments of 4 μ_B.

For **b**, the Cr atom is coupled ferromagnetically with three Ge atoms resulting in a total magnetic moment of 6 μ_B. For the WGe_4, reported calculations[8] show that a pyramidal W-doped Ge_4 structure is formed after one new germanium atom is capped on the quasi-planar rhombus frame. For $CuGe_4$ and $NiGe_4$[6,7] their ground state structures are quite similar with that of $CrGe_4$.

The ground state of $CrGe_4^+$ **a**+ is in a sextet spin manifold. In the planar C_s molecular geometry here, the Ge atoms form a planar rhombus frame, whereas the Cr atom is found to be

TABLE 1: Natural Charge Populations (in e), SOMO(H)−LUMO Gaps (in eV), and Dipole Moment of the Ground-State Structures of $CrGe_n$ and $CrGe_n^+$ ($n = 1-5$)

cluster	natural population	SOMO(H)−LUMO gap	dipole moment	cluster	natural population	SOMO(H)−LUMO gap	dipole moment
CrGe ($^5\Pi$)	0.12	1.65	2.48	$CrGe^+$ ($^6\Sigma$)	0.61	2.11	2.77
$CrGe_2$ ($^5A_1$)	0.45	1.36	3.87	$CrGe_2^+$ ($^4B_1$)	0.60	2.39	3.87
$CrGe_3$ ($^5A_1$)	0.59	1.09	4.15	$CrGe_3^+$ ($^4B_2$)	0.76	1.79	5.20
$CrGe_4$ ($^5B_2$)	0.52	1.66	5.45	$CrGe_4^+$ ($^6A'$)	0.79	2.21	5.44
$CrGe_5$ ($^7A'$)	0.56	1.63	3.66	$CrGe_5^+$ ($^6A_1$)	0.72	2.41	3.90

bridging two Ge atoms. The pyramidal isomer **b**+ and **c**+ are 0.27 and 0.59 eV higher in energy with respect to the ground state. The electronic configuration of **b**+ is the following.

$^6A_1$: ...$(9a_1)^2(4b_2)^2\,(3b_1)^2(1a_2)^2(4b_1)^1(10a_1)^1(2a_2)^1(11a_1)^1(5b_2)^1$.

It results from the removal of an electron from the $5b_2$ orbital of **a**. The B3LYP/TZVP optimized geometry parameters also predicted that **b**+ is an energetically higher-lying species, with an energy gap that amounts to 0.26 eV with respect to **a**+. For the latter **a**+, the Cr atom is found antiferromagnetically coupled with two neighboring Ge atoms, whereas the other two Ge atoms have parallel spin.

$CrGe_5$ and $CrGe_5^+$. An extensive amount of isomers have been located for $CrGe_5$ and $CrGe_5^+$. Only the energetically lower-lying isomers are discussed hereafter. For $CrGe_5$, all of the low-energy isomers listed in Figure 4 possess nonplanar geometries, except for isomer **f**, whose energy lies 1.06 eV above the ground $^7A'$ state **a**. For $CrGe_5^+$, all of the low-energy isomers are characterized as having nonplanar structures. In comparison with the higher homologues WGe_5, the W-capped rhombic pyramidal Ge_5 structure with C_{4v} symmetry was located to be the most stable isomer, whereas for Cu- and Ni-doped Ge_5 clusters, the dominant geometries are the TM-capped bent rhombic pyramidal Ge_n clusters without symmetry (C_1).[6−8] The Cr and five Ge atoms are thus coupled ferromagnetically in both **a** and **a**+ forms, yielding the total magnetic moments of 6 and 5 μ_B, respectively. The natural population analyses indicate that the removed electron from **a**+ ($^6A_1$) has previously occupied the 4p valence orbital of the germanium atom, situated at the apex. On the one hand, the $CrGe_5$ isomer **b** (C_{3v}) is about 0.61 eV higher in energy, as compared to the ground state, and its total magnetic moment amounts to 6 μ_B. On the other hand, for all other low-energy isomers, the total magnetic moment is only $4\mu_B$. Among the $CrGe_5^+$ clusters, the isomer **b**+ is thus situated at 0.42 eV higher than the ground state. The total magnetic moments for the isomers **b**+, **c**+, **d**+, and **f**+ are 5 μ_B, but for **e**+, a smaller value of $3\mu_B$ was obtained.

Averaged Binding Energy and Fragmentation Energy. The averaged binding and fragmentation energies of the $TMGe_n$ (TM = Cu, Ni, W) clusters have been used to predict the relative stability of the doped clusters. The averaged binding energies, defined as E_b and E_b^+, and fragmentation energies as D and D^+ of the $CrGe_n$ and $CrGe_n^+$ clusters can be evaluated according to the following expressions:

$$E_b(n) = [E_T(Cr) + nE_T(Ge) - E_T(CrGe_n)]/n + 1$$

$$D(n, n-1) = E_T(CrGe_{n-1}) + E_T(Ge) - E_T(CrGe_n)$$

$$E_b^+(n) = [E_T(Cr^+) + nE_T(Ge) - E_T(CrGe_n^+)]/n + 1$$

$$D^+(n, n-1) = E_T(CrGe_{n-1}^+) + E_T(Ge) - E_T(CrGe_n^+)$$

where $E_T(CrGe_n)$, $E_T(CrGe_{n-1})$, $E_T(CrGe_n^+)$, $E_T(CrGe_{n-1}^+)$, $E_T(Cr^+)$, $E_T(Cr)$, and $E_T(Ge)$ represent the total energies of the ground states of $CrGe_n$, $CrGe_{n-1}$, $CrGe_n^+$, $CrGe_{n-1}^+$, Cr^+, Cr, and Ge, respectively.

In order to discuss the influence of the doped chromium, we have also calculated the E_b and D of the Ge_n clusters ($n = 2-5$) by the following formulas:

$$E_b(n) = [nE_T(Ge) - E_T(Ge_n)]/n$$

$$D(n, n-1) = E_T(Ge_{n-1}) + E_T(Ge) - E_T(Ge_n)$$

To emphasize the size dependence for the averaged bonding energies and the fragmentation energies of the $CrGe_n$ and $CrGe_n^+$ clusters considered, the calculated results are tabulated as graphical representations shown in Figures 5 and 6.

For both the neutral $CrGe_n$ and cationic $CrGe_n^+$ clusters, the averaged binding energy tend to increase as the number of Ge atoms increases from 1 to 5. The bonding energy of $CrGe_n^+$ is slightly lower than that of corresponding $CrGe_n$, when n ranges from 1 to 3. The bonding energies of $CrGe_n$ are almost equal with that of their cations, when n is equal to 4 and 5. The average bonding energies of $CrGe_4^{(+)}$ and $CrGe_5^{(+)}$ are thus slightly smaller than those of the pure Ge_4 and Ge_5 clusters. This phenomenon was also found for $CuGe_4$ and $CuGe_5$ clusters,[6] but not in WGe_4 and WGe_5 clusters,[8] where the averaged binding energy was reported to be much higher (by almost 1.0 eV) than that of the corresponding pure germanium clusters.

The size dependence for the fragmentation energies of $CrGe_n$ ($n = 1-5$) is very similar to that of the cationic $CrGe_n^+$ counterparts. Similar to the small $CuGe_n$[6] and WGe_n[8] clusters, the fragmentation energies of the $CrGe_n$ clusters are smaller than those of the corresponding values for pure Ge_n clusters when n is 3 and 4 and higher than those of pure germanium clusters when $n = 5$. The local maxima of $D(n, n-1)$ of $CrGe_n^+$ localized with $n = 2$ and 4 imply that the relative stabilities of $CrGe^+$, $CrGe_3^+$, and $CrGe_5^+$ are weaker than those of $CrGe_2^+$ and $CrGe_4^+$.

SOMO−LUMO Energy Gap and Charge Transfer. The energy gap between the highest occupied molecular orbital and the LUMO reflects the chemical stability and the semiconducting character of a cluster. For the ground structures of $CrGe_n$ and $CrGe_n^+$, they have more than two single-occupied molecular orbital, and we only consider energy gap between the highest SOMO and the LUMO. As shown in Table 1, the SOMO−LUMO gaps of $CrGe_3$ and $CrGe_3^+$ are smaller than the corresponding values of other $CrGe_n$ and $CrGe_n^+$ clusters, respectively. The SOMO−LUMO energy gaps of $CrGe_n^+$ are consistently much higher than the corresponding $CrGe_n$ ones.

Previous investigations on the WGe_n clusters indicated that the charges in the WGe_n clusters are transferred from the germanium unit to the W atom and thus contribute to the formation of a hybrid sp^2 germanium cage.[8] However, being different with the WGe_n clusters,[8] the charges in the $CrGe_n$ clusters are always found to be transferred from the Cr atom to the Ge atoms, indicating that the Cr atom acts as an electron

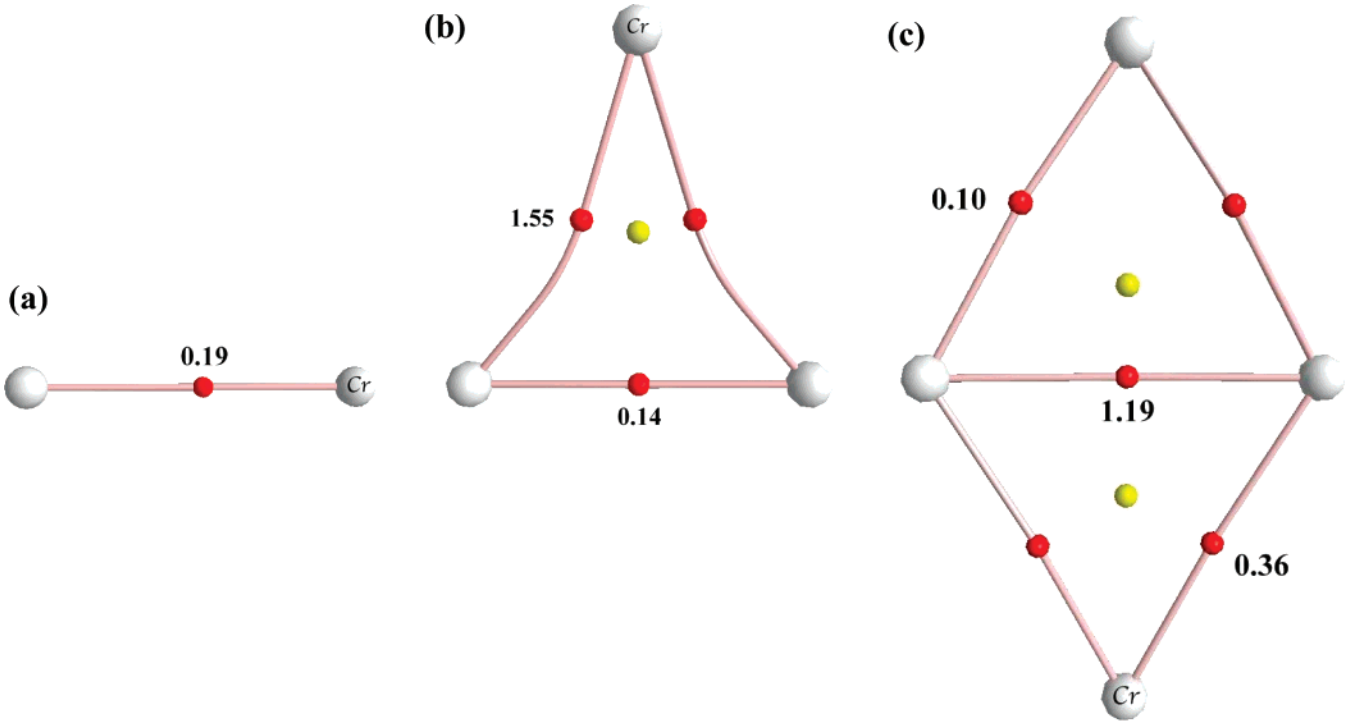

Figure 7. Molecular graphs of CrGe (a), $CrGe_2$ (b), and $CrGe_3$ (c), at its lowest-lying electronic states. Red balls are bcps, yellow balls are rcps and gray balls are germanium atoms, unless otherwise indicated. The ellipticity values of the bcps are also made available.

donor in the $CrGe_n$ clusters. For example, the Cr atom in the ground structure of $CrGe_5$ has a formal $3d^{4.99}4s^{0.42}$ configuration, implying that the electrons in the 4s(Cr) orbital are basically transferred to the 4p(Ge) orbitals. It could be noted that in the Cu-doped Ge clusters,[6] the charges were found to be consistently transferred from the Cu atom to the Ge framework. Such a phenomenon can be explained by the 5d shell saturation of the doped atoms. The 3d orbitals of Cr and Cu atoms are half-filled and completely filled, respectively. For W atom the 5d orbitals tend to accept one electron to become half-filled.

Topology of the Chemical Bonds in $CrGe_2$ and $CrGe_3$. As for a study case, we have considered in the present study the lowest-lying electronic states of $CrGe_2$ and $CrGe_3$. The wavefunctions needed for the AIM analyses have been generated at the B3LYP/6-311++G** level using the Gaussian 03 set of programs.[31] The critical points and the respective bond paths are plotted using the AIM2000 program,[36] and the resulting molecular graphs are illustrated in Figure 7 along with the ellipticity values of the bcps.

For $CrGe_2$, the molecular graph contains three bcps (two Cr−Ge bcps and one Ge−Ge bcp) and one ring critical point (rcp). In the case of $CrGe_3$, we were able to locate five bcps (three Ge−Ge bcps and two Cr−Ge bcps) and two rcps (one Ge−Ge−Ge rcp and one Ge−Ge−Cr rcp). The molecular graph of chromium-doped germanium is quite different from the lithium-doped ones reported earlier;[9,40] indeed the latter lacks the Ge−Ge−Li rcp. The ellipticity is defined as $\epsilon = (\lambda_1/\lambda_2 - 1)$, $\lambda_1 \leq \lambda_2 \leq \lambda_3$, where λ_1, λ_2, and λ_3 are the eigenvalues of the Hessian, and measures the behavior of the electron density in the plane tangential to the interatomic surface at the bcp. The calculated values of the located bcps are also shown in the figure. For the sake of comparison, the molecular graph of Ge−Cr and the respective ellipticity value are also included. The ellipticity values, which range from zero to infinity, can be used as a quantitative index of the π character of a chemical bond. Accordingly, the ellipticity value of the Cr−Ge bcps in $CrGe_2$ is 1.55, whereas a smaller value of 0.19 is obtained for the one in Cr−Ge. A large ellipticity value of the Cr−Ge bcp in $CrGe_2$ suggests a certain π character of the Cr−Ge bond.

The electron density Laplacian's, measured at the respective bcps (defined as $L_b = \nabla^2_{\rho BCP}$), are having small and positive values and similar to that of the lithium-doped species (for Ge−Cr it is 0.01, for $CrGe_2$ it is 0.02, and for $CrGe_3$ it is 0.01).

In an additional approach to characterize the Ge−Cr bond we have used the ELF analysis as adopted for the lithium-doped germanium clusters.[9,40] The ELF isosurfaces and their cut planes plotted for $CrGe_2$ and $CrGe_3$ are shown in Figure 8, and the mean electronic populations computed for each basin are listed in Table 2. In the case of $CrGe_2$, the mean electronic population of the germanium core basins amounts to 27.6 e, and that of chromium sums up to 22.4 e. These values are the sum of the electronic population of all the core basins of respective atoms. The computed C(Ge) populations are of the same order as those in $LiGe_2$. Identical to the lithium-doped diatomic germanium, there exists for $CrGe_2$ a trisynaptic basin, V(Ge1, Ge2, Cr), having an electronic population of 4 e. Note that we were able to locate in the former two such trisynaptic basins (above and below the plane of the molecule) with a total electronic population amounts to 2.65 e.[9] The ELF isosurface of $CrGe_2$ differs largely from that of the $LiGe_2$ counterpart in many other respects, such as the V(Ge) and V(Ge, Ge) basins are absent in the former. In the case of $CrGe_2$, the located V(Ge, Cr) basins are similar to the V(Ge) basins of $LiGe_2$ in its shape; the latter was formally regarded as the lone pair. However, it is a disynaptic basin in $CrGe_2$, and this results leads us to the conclusion that the lone pair like V(Ge) basins contribute significantly toward the Cr−Ge bonding. The electronic populations of the V(Ge,Cr) basins are 3.15 e each and are larger compared to those of the corresponding Li-doped Ge cluster.

The topology of the ELF isosurface of $CrGe_3$ is also considerably different from the Li-doped $LiGe_3$ counterpart. In the former, we were not able to locate a V(Ge,Ge,Ge) trisynaptic basin. Note that our ELF computations derived two disynaptic

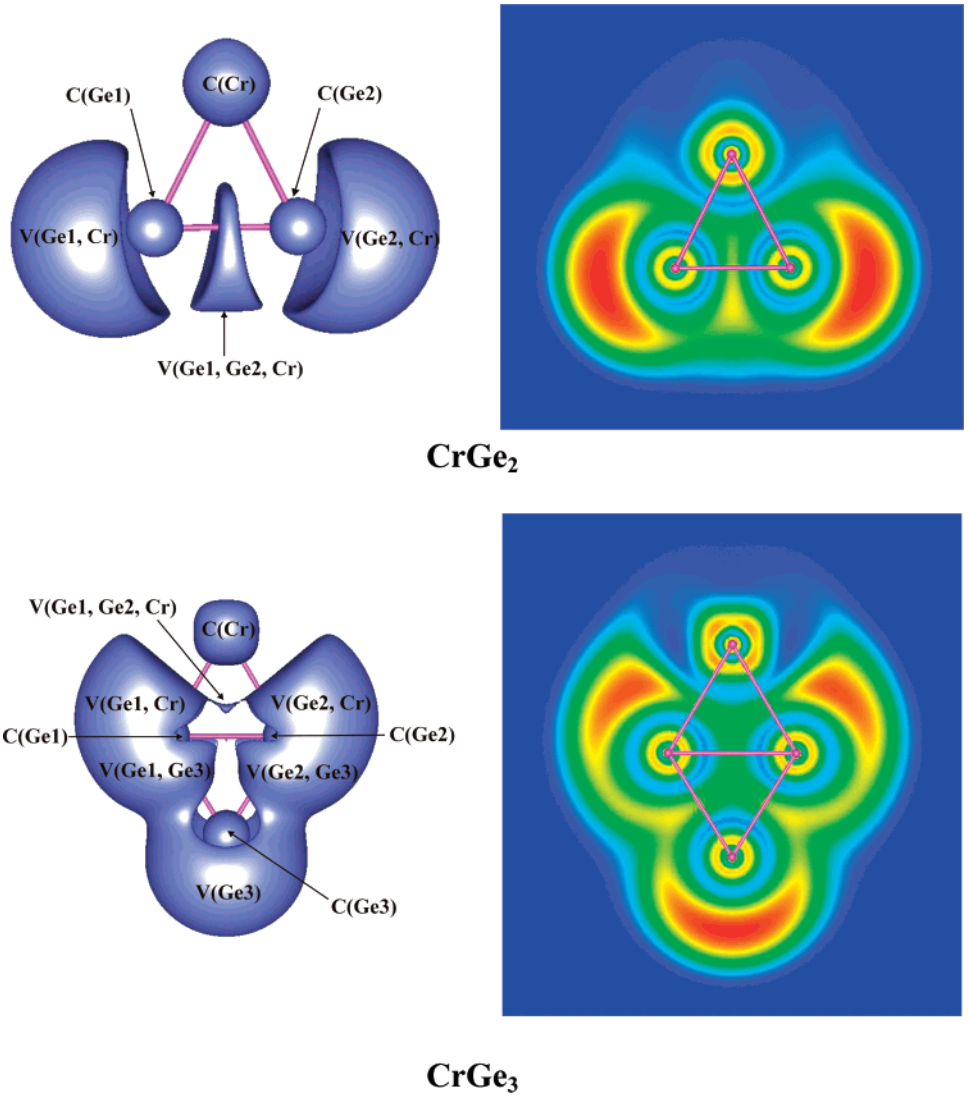

Figure 8. ELF isosurfaces and their cut planes of $CrGe_2$ (isovalue 0.6) and $CrGe_3$ (isovalue 0.49) at its lower-lying electronic states (see Table 2 for the basin populations).

TABLE 2: Mean Electronic Populations Computed for Basins Localized in $CrGe_2$ and $CrGe_3$ and the AIM Charges Obtained by Integrating the Atomic Basins

	molecule		AIM charges	molecule	
basins[a]	$CrGe_2$	$CrGe_3$	atom	$CrGe_2$	$CrGe_3$
C(Ge1)	27.62	27.53			
C(Ge2)	27.62	27.53	Cr	0.39	0.52
C(Ge3)		27.52			
C(Cr)	22.40	22.52	Ge1	−0.19	−0.29
V(Ge1, Cr)	3.15	3.04			
V(Ge1, Ge2, Cr)	4.04	0.60	Ge2	−0.19	−0.29
V(Ge2, Cr)	3.15	3.04			
V(Ge1, Ge3)		2.65	Ge3		0.06
V(Ge2, Ge3)		2.65			
V(Ge3)		2.88			

[a] C stands for core and V stands for valence basins.

V(Ge,Ge) basins, each having an electronic population of 2.65 e. The trisynaptic V(Ge,Ge,Cr) basin with an electronic population of 0.60 e suggests a certain three-center bond in the molecule. Additionally, the occurrence of the V(Ge,Cr) basins suggests a small contribution of Ge lone pair V(Ge) basins toward the Cr−Ge interaction. On the basis of the above analysis of the topology of the ELF isosurfaces, it could be concluded that the bonding in $CrGe_n$ ($n = 2, 3$) is different from that of the respective Li-doped counterpart.

In the present analysis we were also interested in the origin of the high-spin electronic state of Cr−Ge clusters. The main questions we considered here were the followings: (i) Where are the unpaired electrons of $CrGe_n$ ($n = 2, 3$) localized? (ii) How does the Ge−Cr bond differs from the Ge−Li bond? In order to answer these questions, we have adopted a different approach: an ELF analysis by separating the α and β spin components. Such an analysis is expected to give more precise localization of the unpaired electrons as in the case of radicals.[41] The analysis has been performed on the density constructed separating the α and β components of the electron densities for $CrGe_2$ and $CrGe_3$. The density difference between ELF_α and ELF_β isosurfaces are plotted in Figure 9. For further support we have also performed the spin density analyses, and the contour plots are also illustrated in the figure.

For the density difference isosurfaces, defined as

$$\Delta ELF = ELF_\alpha - ELF_\beta$$

the red color indicates the maximum value (or the region where the unpaired electrons are localized), and the blue color corresponds to the minimum value. It is clear from our density difference plots that the unpaired electrons are localized mainly

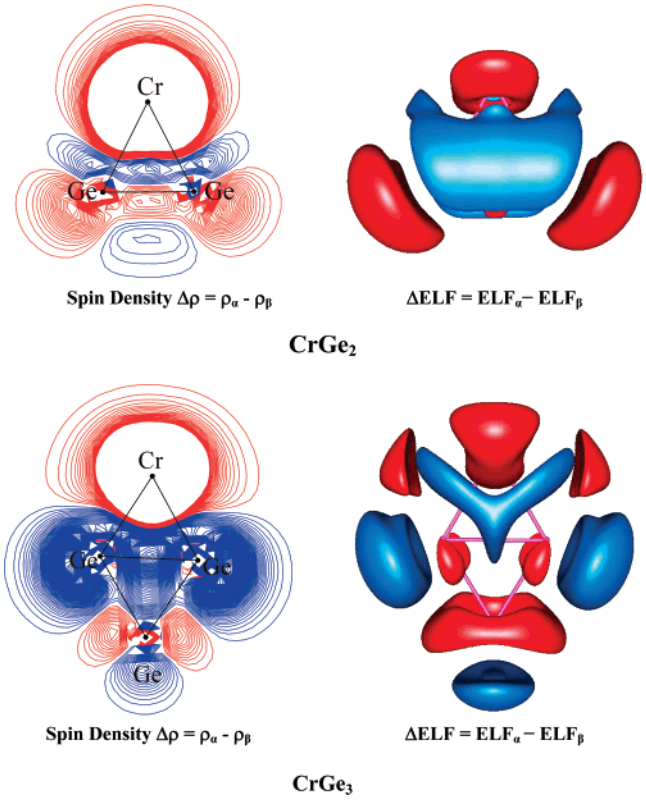

Figure 9. Spin density contour plot (in the plane of the molecule) and isosurfaces of the $\Delta ELF = ELF_\alpha - ELF_\beta$ for $CrGe_2$ (isovalue 0.1 in red and isovalue −0.21 in blue), and $CrGe_3$ (isovalue 0.12 in red and isovalue −0.09 in blue).

on the Cr atoms and partially on the germanium unit. This argument is in agreement with the spin density maps (cf., Figure 9). Note that the isosurfaces of the ΔELF plots and spin density plots are similar in many respects.

Alternately, the electronic structure and bonding can be explained with the help of the qualitative molecular orbital theory. The electronic configuration of the Cr atom is $3d^5 4s^1$, where the entire valence orbitals, the five d and the one s, are singly occupied. The ground state of Ge_2 is triplet ($^3\Sigma_g^-$); the electronic occupation and the shape of the molecular orbitals can be found in ref 9. The unpaired electrons occupy the degenerate π MOs, which are Ge−Ge bonding MOs. The approach of Ge_2 unit toward Cr will be in such a way to facilitate maximum orbital overlap and electron paring. Given the fact that the Ge_2 is at its triplet state, the direction of approach will be along the *x*- or *y*-axis of Cr, in order to maximize the aforementioned conditions. For simplicity, let us postulate that the incoming Ge_2 unit approaches along the *y*-axis with respect to Cr. This leads to an electron pairing in the following two MOs: (i) the MO formed as a result of the overlap between the Cr $4s^1$ orbital with one of the singly occupied π MO of Ge_2 and (ii) the MO resulting from the overlap of d_{yz}^1 orbital of Cr with the degenerate π MO counterpart of Ge_2. This leaves four unpaired electrons in the valence d orbitals of Cr, namely, d_{z^2}, $d_{x^2-y^2}$, d_{xz}, and d_{xy}. Note that the singly occupied d_{xz} and d_{xy} MOs can overlap with the antibonding π MOs of Ge_2 unit, resulting in a d−π back-donation from the Cr atom to the Ge_2 unit. This view is, indeed, supported by the isosurfaces of the ΔELF and spin density plots. In an attempt to further validate the above arguments, we have performed population analysis using the more accurate AIM methodology, and the results are recorded in Table 2. The AIM charges indicate a small positive charge of the amount of 0.39 e on Cr, whereas a negative charge of the amount of −0.19 e is derived for each of the Ge's.

A similar argument can be proposed to rationalize the bonding mechanism in $CrGe_3$. The ground state of Ge_3 is closed shell singlet $^1A_1$, and the lowest-lying triplet state $^3A_1'$ lies 17 kcal mol^{-1} above the ground state.[40] For the electronic occupation and the shape of the MOs, we refer to the ref 40. In the case of $^3A_1'$, the $2b_2$ and $4a_1$ MOs are singly occupied, whereas in the case of the ground state, the former MO is completely filled and the latter is simply vacant. Again, the approach of the Ge_3 unit will be through the *x*- or *y*-axis with respect to Cr in order to maximize the orbital overlap and electron pairing. The former criterion is satisfied by an axial approach (either through the *x*- or *y*-axis), whereas the latter criterion needs the $2b_2$ and $4a_1$ MOs in the Ge_3 unit to be singly occupied. This is due to the symmetry reasons; the d_{xy}^1 and $4s^1$ AOs of the Cr atom can combine with the $2b_2$ and $4a_1$ MOs of the Ge_3 unit resulting in the formation of the molecular orbitals, and the maximum pairing is possible only if the latter MOs are singly occupied (note that all the Cr valence AOs are singly occupied). For that reason, we postulate that the reaction channel for the interaction of Ge_3 with Cr is likely to proceed via an electronically excited triplet state of Ge_3. This will, indeed, leave the four unpaired electrons in the d orbitals of Cr, namely, in d_{z^2}, $d_{x^2-y^2}$, d_{xz}, and d_{yz} (assuming that the direction of approach of the Ge_3 unit is along the *y*-axis with respect to the Cr atom). Again, due to symmetry reason, an overlap is possible between the singly occupied d_{xz} and d_{yz} AOs of Cr atom and the vacant $1a_2$ and $2b_1$ antibonding π MOs of the Ge_3 unit. And this will result in a small amount of d−π back-donation from Cr to the Ge_3 unit. Similar to the case of $CrGe_2$ the population analysis suggests a small positive charge of the amount of 0.52 e on the Cr atom and a small negative charge of −0.29 e on each of the Ge atoms bonded to the Cr. The isosurfaces of the ELF density difference and spin density plots supports the above argument. The π character of the Ge−Cr bond in both of the molecules is well reflected in the calculated large ellipticity values of the Ge−Cr bcps reported in the first section.

Conclusions

In the present work, based on our computational analysis we are able to draw the following conclusions:

(i) For the neutral and cationic $CrGe_n$ clusters with $n = 2-4$, the ground state structures are planar, except for the neutral $CrGe_4$. Both neutral and cationic $CrGe_5$ forms are nonplanar.

(ii) The fragmentation energies of the $CrGe_n$ clusters are smaller than those of the corresponding values for pure Ge_n clusters when *n* is equal to 3 and 4 and higher than those of pure germanium clusters when $n = 5$. The Cr atom acts as an electron donor in the $CrGe_n$ clusters.

(iii) The electronic structure and bonding mechanism in $CrGe_2$ and $CrGe_3$ have been investigated using AIM and ELF analysis. Our ELF computations suggest that the bonding in chromium-doped germanium clusters is different in many aspects from that of the lithium-doped clusters.

(iv) For $CrGe_n$ with $n = 2$ and 3, a small amount of d−π back-donation is anticipated within the framework of the proposed bonding model.

(v) The density difference plots for $\Delta ELF = ELF_\alpha - ELF_\beta$ are in agreement with the spin density results and support the proposed chemical bonding model using the MO theory, i.e., the axial approach of the Ge_n ($n = 2, 3$) unit and the d−π back-donation.

Acknowledgment. The authors are indebted to the KU Leuven Research Council (GOA program) and the Flemish Fund for Scientific Research (FWO-Vlaanderen) for continuing support. The authors also warmly thank Professor Patricio Fuentealba for valuable comments regarding the ELF_α and ELF_β computations.

Supporting Information Available: All structures found for the neutral and cationic $CrGe_n^{0,+}$ ($n = 2-5$) clusters. This material is available free of charge via the Internet at http://pubs.acs.org.

References and Notes

(1) Kawamura, H.; Kumar, V. *Phys. Rev. B* **2004**, *70*, 245433 and references therein.
(2) Jarrold, M. F.; Bower, J. E. *J. Chem. Phys*. **1992**, *96*, 9180.
(3) (a) Lu, J.; Nagase, S. *Chem. Phys. Lett.* **2003**, *372*, 394. (b) Singh, A. K.; Kumar, V.; Kawazoe, Y. *Eur. Phys. J.: Appl. Phys.* **2005**, *34*, 295; *Phys. Rev. B* **2005**, *71*, 075312.
(4) (a) Kumar, V.; Kawazoe, Y. *Phys. Rev. Lett.* **2002**, *88*, 235504; (b) Kumar, V.; Kawazoe, Y. *Appl. Phys. Lett.* **2002**, *80*, 859.
(5) Akutsu, M.; Koyasu, K.; Atobe, J.; Miyajima, K.; Mitsui, M.; Nakajima, A. *J. Phys. Chem. A* **2007**, *111*, 573.
(6) Wang, J.; Han J. G. *J. Chem. Phys.* **2005**, *123*, 244303 and references therein.
(7) Wang, J.; Han, J. G. *J. Phys. Chem. B* **2006**, *110*, 7820.
(8) Wang, J.; Han, J. G. *J. Phys. Chem. A* **2006**, *110*, 12670.
(9) Gopakumar, G.; Lievens, P.; Nguyen, M. T. *J. Chem. Phys.* **2006**, *124*, 214312.
(10) Jarrold, M. F. *Science*, **1991**, *252*, 1085.
(11) Raghavachari, K.; Curtiss, L. A. *Quantum Mechanical Electronic Structure Calculations with Chemical Accuracy*; Kluwer Academic: The Netherlands, 1995.
(12) Arnold, C. C.; Xu, C.; Burton, G. R.; Neumark, D. M. *J. Chem. Phys.* **1995**, *102*, 6982.
(13) (a) Burton, G. R.; Xu, C.; Arnold, C. C.; Neumark, D. M. *J. Chem. Phys.* **1996**, *104*, 2757. (b) Burton, G. R.; Xu, C.; Neumark, D. M. *Surf. Rev. Lett.* **1996**, *3*, 383.
(14) Cheshnovsky, O.; Yang, S. H.; Pettiette, C. L.; Craycraft, M. J.; Liu, Y.; Smalley, R. E. *Chem. Phys. Lett.* **1987**, *138*, 119.
(15) (a) Gingerich, K. A.; Finkbeiner, H. C.; Schmude, R. W., Jr. *J. Am. Chem. Soc.* **1994**, *116*, 3884. (b) Gingerich, K. A.; Shim, I.; Guptha, S. K.; Kingcade, J. E. *Surf. Sci.* **1985**, *156*, 495.
(16) Kingcade, J. E.; Choudary, U. V.; Gingerich, K. A. *Inorg. Chem.* **1979**, *18*, 3094.
(17) Negishi, Y.; Kawamata, H.; Hayase, T.; Gomei, M.; Kishi, R.; Hayakawa, F.; Nakajima, A.; Kaya, K. *Chem. Phys. Lett.* **1997**, *269*, 199.
(18) Xu, C.; Taylor, T. R.; Burton, G. R.; Neumark, D. M. *J. Chem. Phys.* **1998**, *108*, 1395.
(19) Jackson, P.; Fisher, K. J.; Gadd, G. E.; Dance, I. G.; Smith, D. R.; Willett, G. D. *Int. J. Mass Spectrom. Ion Processes* **1997**, *164*, 45.
(20) Dai, D.; Balasubramanian, K. *J. Chem. Phys.* **1996**, *105*, 5901.
(21) Balasubramanian, K. *Chem. Rev.* **1990**, *90*, 93.
(22) Dixon, D. A.; Gole, J. L. *Chem. Phys. Lett*. **1992**, *188*, 560.
(23) Lanza, G.; Millefiori, S.; Millefiori, A. *J. Chem. Soc., Faraday Trans.* **1993**, *89*, 2961.
(24) Archibong, E. F.; St-Amant, A. *J. Chem. Phys.* **1998**, *109*, 962.
(25) Deutsch, P. W.; Curtiss, L. A.; Blaudeau, J. P. *Chem. Phys. Lett.* **1997**, *270*, 413.
(26) Ogut, S.; Chelikowsky, J. R. *Phys. Rev. B* **1997**, *55*, R4914.
(27) Neukermans, S.; Wang, X.; Veldeman, N.; Janssens, E.; Silverans, R. E.; Lievens, P. *Int. J. Mass Spectom.* **2006**, *252*, 145.
(28) (a) Becke, A. D. *J. Chem. Phys.* **1996**, *104*, 1040. (b) Lee, C. T.; Yang, W. T.; Parr, R. G. *Phys. Rev. B* **1988**, *37*, 785. (c) Miehlich, B.; Savin, A.; Stoll, H.; Preuss, H. *Chem. Phys. Lett.* **1989**, *157*, 200.
(29) Hay, P. J.; Wadt, W. R. *J. Chem. Phys.* **1985**, *82*, 270; **1985**, *82*, 284; **1985**, *82*, 299.
(30) Shim, I.; Sai Baba, M.; Gingerich, K. A. *Chem. Phys.* **2002**, *277*, 9.
(31) Frisch, M. J.; Trucks, G. W.; Schlegel, H. B.; Scuseria, G. E.; Robb, M. A.; Cheeseman, J. R.; Montgomery, J. A., Jr.; Vreven, T.; Kudin, K. N.; Burant, J. C.; Millam, J. M.; Iyengar, S. S.; Tomasi, J.; Barone, V.; Mennucci, B.; Cossi, M.; Scalmani, G.; Rega, N.; Petersson, G. A.; Nakatsuji, H.; Hada, M.; Ehara, M.; Toyota, K.; Fukuda, R.; Hasegawa, J.; Ishida, M.; Nakajima, T.; Honda, Y.; Kitao, O.; Nakai, H.; Klene, M.; Li, X.; Knox, J. E.; Hratchian, H. P.; Cross, J. B.; Bakken, V.; Adamo, C.; Jaramillo, J.; Gomperts, R.; Stratmann, R. E.; Yazyev, O.; Austin, A. J.; Cammi, R.; Pomelli, C.; Ochterski, J. W.; Ayala, P. Y.; Morokuma, K.; Voth, G. A.; Salvador, P.; Dannenberg, J. J.; Zakrzewski, V. G.; Dapprich, S.; Daniels, A. D.; Strain, M. C.; Farkas, O.; Malick, D. K.; Rabuck, A. D.; Raghavachari, K.; Foresman, J. B.; Ortiz, J. V.; Cui, Q.; Baboul, A. G.; Clifford, S.; Cioslowski, J.; Stefanov, B. B.; Liu, G.; Liashenko, A.; Piskorz, P.; Komaromi, I.; Martin, R. L.; Fox, D. J.; Keith, T.; Al-Laham, M. A.; Peng, C. Y.; Nanayakkara, A.; Challacombe, M.; Gill, P. M. W.; Johnson, B.; Chen, W.; Wong, M. W.; Gonzalez, C.; Pople, J. A. *Gaussian 03*, revision B.03; Gaussian, Inc.: Wallingford, CT, 2003.
(32) Hou, X.-J., Nguyen, M. T. To be published.
(33) Schafer, A.; Huber, C.; Ahlrichs, R. R. *J. Chem. Phys.* **1994**, *100*, 5829.
(34) *ADF 2005.01*; SCM/Vrije Universiteit Amsterdam, Theoretical Chemistry: Amsterdam, The Netherlands.
(35) (a) Bader, R. F. *Atoms in Molecules: A Quantum Theory*; Oxford University Press: New York, 1995. (b) Popelier, P. *Atoms in Molecules: An Introduction*; Prentice Hall: New York, 2000.
(36) Biegler-König, F.; Schönbohm, J.; Bayles, D. AIM2000—A Program to Analyze and Visualize Atoms in Molecules. *J. Comput. Chem.* **2001**, *22*, 545.
(37) (a) Becke, A. D.; Edgecombe, K. E. *J. Chem. Phys.* **1990**, *92*, 5397. (b) Silvi, B.; Savin, A. *Nature* **1994**, *371*, 683. (c) Kohout, M. *Int. J. Quantum Chem.* **2004**, *97*, 651. (d) Kohout, M.; Wagner, F. R.; Grin, Y. *J. Phys. Chem. A* **2002**, *108*, 150.
(38) Noury, S.; Krokidis, X.; Fuster, F.; Silvi, B. *TopMod Package*; Université Pierre et Marie Curie: Paris, 1998.
(39) (a) Laaksonen, L. J. *J. Mol. Graphics* **1992**, *10*, 33. (b) Bergman, D. L.; Laaksonen, L.; Laaksonen, A. *J. Mol. Graphics Modell.* **1997**, *15*, 301.
(40) Gopakumar, G.; Lievens, P.; Nguyen, M. T. *J. Phys. Chem. A* **2007**, *111*, 4353.
(41) Melin, J.; Fuentealba, P. *Int. J. Quantum Chem.* **2003**, *92*, 381.